

Parity issues, stress results, and oscillator strengths of the rotational tunneling (H,Be) and (D,Be) complexes in silicon: The rigid rotor in a tetrahedral field

Kevin R. Martin* and W. Beall Fowler

Department of Physics and Sherman Fairchild Laboratory, Lehigh University, Bethlehem, Pennsylvania 18015

(Received 11 August 1995)

We apply a model of a rigid rotor in a tetrahedral field to the (H,Be) and (D,Be) complexes in silicon. The issue of $\langle 111 \rangle$ versus $\langle 100 \rangle$ minima is explored within this model, with the latter gaining support for these complexes. It is then shown that parity is nearly a good quantum number for the wave functions when the minima are in $\langle 100 \rangle$ directions, even though the Hamiltonian is invariant under operations of the group T_d . We then calculate the stress effects on the levels within this model, refuting the notion that [111] stress has no effect when the minima are in six $\langle 100 \rangle$ directions. The stress effects for the small basis-set tetrahedral tunneling model are recalculated, and it is found that conclusions that had been drawn must be reevaluated. Also, we present formulas for stress effects in the small basis-set octahedral tunneling model. Finally, a coupling scheme is developed by using symmetry arguments, and oscillator strengths are calculated for transitions in both the infrared (hole transition plus rotational sidebands) and far-infrared (coupled rotational transitions).

I. INTRODUCTION

There have been two experiments to date on the (H,Be) and (D,Be) single acceptor complexes in silicon, both of which indicate that these two complexes are hindered rotors, or in a more extreme limit, tunneling systems. Muro and Sievers explored the temperature dependence of the infrared (IR) spectra and the low-temperature far-infrared (FIR) spectra of these two complexes in silicon.¹ They found that at 1.7 K these complexes have, in addition to normal single acceptor IR absorption lines ("p_{3/2} series," and labeled in their paper by *I*) a blueshifted replica (labeled *I*^{*}) of each line positioned at 38.7 and 16.2 cm⁻¹ higher in energy relative to the main band for the hydrogen and deuterium isotope, respectively.¹ As they increased the temperature, additional redshifted replicas (labeled by *II*, *III*, etc.) appeared in the IR absorption, indicating a complex manifold of levels in the ground state more closely spaced than the blueshifted replicas. Directed transitions between these levels were also seen by Muro and Sievers using FIR techniques.¹

Peale, Muro, and Sievers also saw a normal single acceptor absorption line (labeled by *I*) at higher energy corresponding to the strongest transition of the so-called p_{1/2} series, also with blueshifted replicas (labeled *I*^{*}) at a slightly more accurate 38.8 cm⁻¹ for the hydrogen isotope and again at 16.2 cm⁻¹ for the deuterium isotope.² As they raised the temperature, redshifted peaks again became apparent, agreeing with Muro and Sievers. Additional information was obtained by monitoring the effect of uniaxial stress on the transitions. The largest shift of the transitions themselves at 1.7 K was seen for [111] stress, with a smaller shift for [110] stress, and the smallest shift for [001] stress, for both isotopes. At the elevated temperature of 6 K, evidence for a stress-split ground level was seen, indicating that the ground level transforms as Γ_8 , since this is the only irreducible representa-

tion in T_d that can split, due to a reduction in symmetry by uniaxial stress.² This is the same symmetry as the ground level of an ordinary single acceptor.

The following conceptual view is used to frame the experimental results. When doped into silicon, Be occupies a substitutional site and is a double acceptor. When hydrogen or deuterium is introduced, a complex with Be is formed partially passivating the double acceptor. The composite system is then a single acceptor with the possibility of an additional degree of freedom of hindered rotational motion (also vibrational) or possibly, if the potential wells are sufficiently deep, rotational tunneling.

Initially, a model developed by Haller, Joos, and Falicov for a different defect³ was used to model these complexes. For the rotational tunneling motion, a simple four-dimensional Hilbert space is assumed, spanned by identical functions oriented along four $\langle 111 \rangle$ directions (either bonding or antibonding directions). This tetrahedral tunneling model predicts two tunneling levels, A_1 and T_2 , separated by $4t$ in energy, where $-t$ is the tunneling matrix element.³ For the ground state of the single acceptor, which has an *s*-like envelope wave function, coupling between the rotational tunneling nuclei and the single acceptor hole may be significant, so Haller, Joos, and Falicov³ developed a two parameter coupling scheme, which predicts five levels in the ground-state manifold.³ Hence, the blueshifted replicas were interpreted within this tetrahedral tunneling model as a transition from the common ground state to the excited single acceptor state with T_2 nuclear tunneling character, and the redshifted replicas were interpreted as a result of the five coupled levels.^{1,2} The model was applied, seemingly satisfactorily, by both sets of experimentalists to these complexes. However, several serious difficulties exist, one of which is fatal. As first pointed out by Peale, Muro, and Sievers, the energy values of the blueshifted replicas relative to the main band are larger than the free

rotor limit for these complexes.² Free rotation should be the upper limit, since any interaction with the surrounding crystalline environment will only “drag” the rotor, and hence will decrease the spacing between the levels.⁴ As we will see, there are also problems in applying this tetrahedral tunneling model to the experimental stress results.

Artacho and Falicov introduced a similar model, except that they assumed a six-dimensional Hilbert space for the rotational tunneling nuclei corresponding to six identical $\langle 100 \rangle$ oriented functions (C sites).⁵ This model predicts three nuclear tunneling levels, A_{1g} , T_{1u} , and E_g , in which the separation between the A and T levels is twice that of the separation of the T and E levels. Again, a two-parameter coupling scheme was developed, introducing eight levels in the ground-state manifold. It was assumed in this octahedral tunneling model that the system is invariant under operations of the group O_h , so that parity is exactly a good quantum number.⁵ This is apparently inconsistent with the assumption that the complexes are at a substitutional site, since the point symmetry there should be T_d , but Artacho and Falicov argued that parity in the total wave function may be nearly a good quantum number in the actual system if crystal-field corrections arising from neighboring Si atoms are neglected,⁵ since the hole states are described by the product of a smooth envelope of s - or p -like character and linear combinations of the six spinors from the top of the valence band. If this is the case, then the blueshifted replicas seen in the experiments are a result of a transition from the common ground state with predominantly A_{1g} tunneling character to the excited acceptor state with E_g tunneling character, since a sideband transition of this nature (from s - to p -like acceptor states) will probe the *like* parity of the tunneling states. If parity were exactly a good quantum number, as it is in Artacho and Falicov’s octahedral tunneling model, then a sideband transition to the intermediate T_{1u} tunneling state would be identically zero. This model would eliminate the problem encountered in the tetrahedral tunneling model, because in the free rotor limit, the E_g level would originate from the $L=2$ free rotor level, which has a larger energy spacing relative to the $L=0$ free rotor level than the blueshifted replicas seen experimentally. The absence of several absorption lines seen in the FIR spectra could also be explained by noting that a transition within the ground-state manifold (within the s -like acceptor states) probes the *opposite*-parity characteristics of the tunneling states, so that only four of the possible seven transitions predicted by this octahedral tunneling model are allowed.⁵

There is some theoretical support for $\langle 100 \rangle$ minima. The pseudopotential-density-functional calculations of Denteneer, Van de Walle, and Pantelides,⁶ calculations of Chia, Goh, and Ong,⁷ and the *ab initio* pseudopotential total-energy method calculations of Lee, Cheong, and Chang⁸ all indicated global minima at or near the six $\langle 100 \rangle$ directions (C site).

However, there are issues concerning the octahedral tunneling model that will have to be addressed. One issue is that no attempt has been made to reconcile this

model with the observed stress results of Peale, Muro, and Sievers.² In fact, it is intuitive that $[001]$ stress should have the “largest” effect, with $[111]$ stress the least, apparently contradictory to the experimental result. A second major issue concerning this model is that of parity. The complexes must have T_d symmetry if located at a substitutional site. Finally, both the tetrahedral and octahedral tunneling models are small basis models, which if a potential-energy surface were assigned, would have to have deep minima in the direction of interest so that the wave functions could be written as assumed. Hence, the term “tunneling” has been used to describe these models. However, the possibility of “hindered rotation” exists, especially in the case of $\langle 100 \rangle$ minima. A larger basis set would be required to treat accurately hindered rotation.

Our initial calculations treating these complexes as a rigid rotor in a tetrahedral field indicated that any model with $\langle 111 \rangle$ minima must be eliminated.⁴ The suggestion by Artacho and Falicov of $\langle 100 \rangle$ minima⁵ has opened possibilities within our rotor model. This model is more general than the two other models and includes them as limiting cases in the deep-well limit of our parameters.⁹ Indeed, this model allows the investigation of intermediate cases, and it also allows a detailed investigation of assumptions inherent in the other two models. We have found, using the rigid rotor in a tetrahedral field model, that definite statements in regard to parity and uniaxial stress issues can be made. Also, as of the present, only qualitative discussions of the strengths of transitions have been made. We will present quantitative results on the oscillator strengths of the various transitions.

II. THEORETICAL CONSIDERATIONS

A. General formalism

The Hamiltonian for the (H,Be) and (D,Be) complexes in silicon is written as

$$\mathcal{H} = \mathcal{H}_a(\mathbf{r}) + \mathcal{H}_N(\mathbf{R}) + V(\mathbf{r}, \mathbf{R}), \quad (1)$$

where $\mathcal{H}_a(\mathbf{r})$ describes the dynamics of a normal single acceptor, $\mathcal{H}_N(\mathbf{R})$ describes the dynamics of the rotational tunneling nuclei, and $V(\mathbf{r}, \mathbf{R})$ couples the two motions. \mathbf{r} is the coordinate of the hole, and \mathbf{R} is the coordinate of the rotating nuclei (\mathbf{R} can be defined as the relative coordinate of the beryllium and hydrogen or deuterium). All terms will be assumed to be invariant under the operations of the group T_d .

We will have nothing new to add to $\mathcal{H}_a(\mathbf{r})$. It is assumed that the typical approach has been applied to $\mathcal{H}_a(\mathbf{r})$, notably the spherical model with cubic corrections by Baldereschi and Lipari for the envelope states.¹⁰ We assume that we have the energy spectrum of the single acceptor problem, including the corrections for the s -like envelope ground state, with spin-orbit interactions included.

For the other two terms in the Hamiltonian, a detailed model will be developed. We first start with the nuclear rotational part, $\mathcal{H}_N(\mathbf{R})$. \mathcal{H}_N will be treated as a rigid ro-

tor in a tetrahedral field,⁴ in analogy with Devonshire's treatment of the octahedral field.¹¹

We write for \mathcal{H}_N ,

$$\mathcal{H}_N(\mathbf{R}) = B \left\{ \frac{L^2}{\hbar^2} + V(\theta, \phi) \right\}, \quad (2)$$

where $B = \hbar^2/2I$, the rotational constant (I is the moment of inertia μR^2). Notice that V is dimensionless. The corresponding Schrödinger equation is then given by

$$\left[\frac{L^2}{\hbar^2} + V(\theta, \phi) \right] \psi = W \psi, \quad (3)$$

where a dimensionless energy eigenvalue is defined as $W = E/B$, so that everything is scaled according to B . If V were zero, the problem is that of the free rigid rotor, with eigenvalues $(L)(L+1)$ and the eigenvectors would be the spherical harmonics Y_{LM} .

The symmetry of the problem must be carefully discussed. The complex is at a substitutional site, in which the rotation is about some axis, not necessarily around the Be atom or the center of mass. The four-nearest neighbors are tetrahedrally arranged around the rotor, hence constraining the form of $V(\theta, \phi)$ to be invariant under T_d symmetry. It is important to note that the second-nearest neighbors are in 12 $\langle 110 \rangle$ directions, which imposes O_h symmetry. Hence, if a contribution from the second-nearest neighbors is included in V , parity must be a good quantum number for that part of the expansion since the inversion operator is included in O_h .

We choose to expand the potential in spherical harmonics. We then write for V ,

$$V(\theta, \phi) = K (Y_3^{\text{tet}} + C_4 Y_4^{\text{tet}} + C_6 Y_6^{\text{tet}}), \quad (4)$$

where K is the *strength* of the potential, and C_4 and C_6 measure the *shape* of the potential. This is the most general potential allowed by T_d symmetry, except for the truncation of terms with $L > 6$. This is not a point ion expansion, although that connection can be made so that specific values of C_4 and C_6 may be determined.¹² An $L=0$ term should also be present, but since it is a trivial constant, it is subtracted out. We did not previously include the $L=6$ term in our calculations.^{4,9} The Y^{tet} 's are linear combinations of spherical harmonics, which transform as A_1 in T_d , and are given as

$$\begin{aligned} Y_3^{\text{tet}} &= \frac{3}{7} \sqrt{40\pi/7} i \{ Y_{32} - Y_{3-2} \}, \\ Y_4^{\text{tet}} &= -\sqrt{4\pi/9} \{ Y_{40} + \frac{1}{2} \sqrt{\frac{10}{7}} (Y_{44} + Y_{4-4}) \}, \\ Y_6^{\text{tet}} &= \sqrt{4\pi/13} \{ Y_{60} - \sqrt{\frac{7}{2}} (Y_{64} + Y_{6-4}) \}. \end{aligned} \quad (5)$$

The size of each of these terms can be gauged by squaring (complex conjugate) and integrating over all space, and finally taking the square root of the result. For the $L=3, 4,$ and 6 terms, we find that the values are approximately 2.568, 1.547, and 2.781, respectively. The normalizations of the Y^{tet} 's are essentially arbitrary, although the $L=4$ term is chosen so that it is identical to Devonshire's potential.¹¹

The above expressions can be rewritten in terms of angles,

$$\begin{aligned} Y_3^{\text{tet}} &= -15 \frac{\sqrt{3}}{7} \cos(\theta) \sin^2(\theta) \sin(2\phi), \\ Y_4^{\text{tet}} &= -\frac{1}{8} [3 - 30 \cos^2(\theta) + 35 \cos^4(\theta) \\ &\quad + 5 \sin^4(\theta) \cos(4\phi)], \\ Y_6^{\text{tet}} &= \frac{1}{16} \{ -5 + 105 \cos^2(\theta) - 315 \cos^4(\theta) + 231 \cos^6(\theta) \\ &\quad - 21[-1 + 11 \cos^2(\theta)] \sin^4(\theta) \cos(4\phi) \} \end{aligned} \quad (6)$$

or finally in Cartesian form

$$\begin{aligned} Y_3^{\text{tet}} &= -30 \frac{\sqrt{3}}{7} \frac{xyz}{r^3}, \\ Y_4^{\text{tet}} &= -\frac{1}{2} \left\{ \frac{5}{r^4} (x^4 + y^4 + z^4) - 3 \right\}, \\ Y_6^{\text{tet}} &= \frac{1}{2r^6} \{ 7(x^6 + y^6 + z^6) - 5(x^2 + y^2 + z^2)^3 \\ &\quad + 210x^2y^2z^2 \}. \end{aligned} \quad (7)$$

We choose as basis functions the spherical harmonics, and in all that follows up to and including $L=15$ (256 by 256) are included in the expansion. The eigenvalue spectrum of Eq. (3) with $C_6=0$ has been published elsewhere,^{4,9} and evaluated in more detail (with C_6 other than zero).¹² To make phrases somewhat clearer that have been used and will be used throughout this paper and the literature, for a given C_4 and C_6 , the phrases "free rotor," "hindered rotor," "rotational tunneling," and "libration" mean, from our perspective, increasing K from zero to very large. The specific values of K that separate the various regions of motion are not rigid, but the general use of these phrases should be understood. The potential as written, and indeed in the general T_d case, predicts three possible sets of minima; the four bonding $\langle 111 \rangle$ directions, the four antibonding $\langle 111 \rangle$ directions, and the six $\langle 100 \rangle$ directions.^{4,12} We will be interested only in the case when the minima, shallow or not, are in the six $\langle 100 \rangle$ directions. This severely restricts the parameter space which we will need to investigate. In particular, K will be positive.

B. Parity considerations for the nuclear Hamiltonian

As pointed out in the Introduction, if parity were a good quantum number, or at least nearly so, then it would be possible to explain the blueshifted replicas experimentally seen since a sideband transition to the third nuclear hindered rotational level would be responsible for the absorption. We wish now to devise a method for determining to what degree the eigenfunctions of the hindered rotational levels in our rigid-rotor model are even or odd.

Clearly, there are two limits of the potential of Eq. (4), which will generate eigenfunctions that are exactly even or odd. The trivial limit $K=0$ increases the symmetry of

the Hamiltonian to the full rotation group, so that the eigenfunctions are simply s , p , d , etc. states, which are even or odd. The other limit occurs when $C_4 \rightarrow \infty$ and/or $C_6 \rightarrow \infty$ as $K \rightarrow 0$, so that KC_4 and/or KC_6 remains finite. This essentially amounts to dropping the $L=3$ term in the potential. Since the $L=4$ and 6 terms have even parity, the eigenfunctions must be even or odd. As discussed before, these two terms in the potential are invariant under O_h symmetry, which has even and odd representations. However, we are more interested in whether parity is nearly a good quantum number for reasonable values of the parameters, meaning that C_4 and C_6 are relatively small, so that the $L=3$ term in the potential has a significant contribution.

We proceed to define a function F as

$$F(\mathbf{r}) = \frac{\psi(\mathbf{r}) - \psi(-\mathbf{r})}{2}, \quad (8)$$

where ψ is an arbitrary function. Clearly, F is the odd part of ψ . If we multiply F by its complex conjugate and integrate over all space, the result is

$$\int |F|^2 d\mathbf{r} = \frac{1}{2} \left\{ 1 - \text{Re} \int \psi^*(\mathbf{r})\psi(-\mathbf{r}) d\mathbf{r} \right\}, \quad (9)$$

where "Re" means take the real part. We define the right side of Eq. (9) to be the measure of parity. All the eigenfunctions in the rigid-rotor model must be of the form

$$\psi = \sum_{LM} a_{LM} Y_{LM}, \quad (10)$$

where the Y 's are the spherical harmonics and the a 's are the expansion coefficients. The measure of parity [Eq. (9)] then becomes

$$\text{Parity} = \frac{1}{2} \left\{ 1 - \sum_{LM} |a_{LM}|^2 (-1)^L \right\}. \quad (11)$$

The $(-1)^L$ fact comes from the inversion property of spherical harmonics. Clearly, if the function is exactly odd Eq. (11) gives 1 and if it is exactly even, 0. If both the even and odd parts of ψ have the same integrated strength, Eq. (11) will return a value of 0.5. This measure of parity is simple to calculate.

A typical case is shown in Fig. 1. For the values of the parameters given ($C_4=2.0$, $C_6=0.30$) the six $\langle 100 \rangle$ directions are the global and only minima for positive K , while for negative K the four $\langle 111 \rangle$ directions (bonding directions, by our chosen convention) are the global minima. The first four levels are shown, which include the A_1 derived from the free rotor s state ($L=0$), the T_2 derived from the free rotor p states ($L=1$) and the E and T_2 derived from the free rotor d states ($L=2$).

Clearly in Fig. 1, for all positive K , the three levels (which are lowest in energy) $A_1, T_2(L=1), E$, have parity as nearly a good quantum number. The fourth level, however, is approaching the value of 0.5 for large, positive K , indicating an equal mixing of even and odd spherical harmonics. This fourth level and all four levels for negative K indicate clearly that the symmetry of our

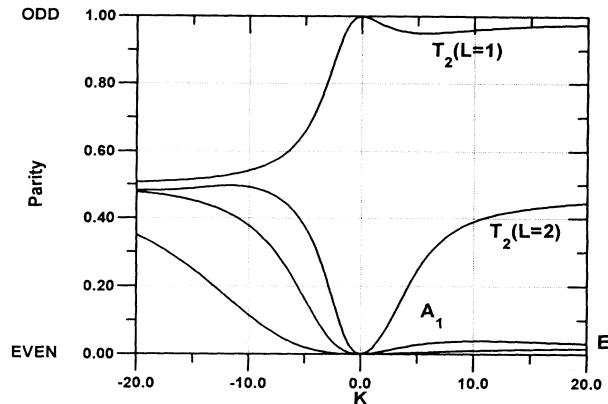


FIG. 1. Parity, as given by Eq. (11), of the first four levels when $C_4=2.0$ and $C_6=0.30$ in the rigid rotor in a tetrahedral field model. A value of "1" means that the function is exactly odd (containing only $L=\text{odd}$ terms in the expansion), while a value "0" means that the function is exactly even (containing only $L=0$ and even terms). The first three levels have parity as nearly a good quantum number for positive K . The parity of the fourth level [$T_2(L=2)$] and all four levels for negative K indicate that the Hamiltonian has T_d symmetry.

Hamiltonian is not O_h but is T_d . We had expected parity in all the eigenfunctions for large values of C_4 and C_6 , but we are seeing parity, at least in the first three levels, even with reasonable values of the parameters. $C_4=2.0$ makes the $L=4$ term in the potential about the same size as the $L=3$ term (using the integrated strength of each term to measure the size of the term), while $C_6=0.3$ makes the $L=3$ term about three times as large as the $L=6$ term.

Artacho and Falicov in their octahedral tunneling model had to justify the O_h symmetry they assumed for the Hamiltonian by neglecting the nearest-neighbor contributions.⁵ They argued that the second-nearest neighbors may play an important role. The reason for doing this is to get the third nuclear rotational level involved in a transition, while a transition to the second level is forbidden. Their arguments seemed unphysical to us. It has now been shown that parity can be a good quantum number, at least for the first three levels, even with a Hamiltonian that is clearly invariant under T_d , not O_h , and not necessarily within a deep-well limit. Artacho and Falicov's suggestion of parity as being a good quantum number was highly intuitive. We have been able to justify it with a general expansion in T_d symmetry.

It is interesting to note that, for silicon, the single acceptor (\mathcal{H}_a) Hamiltonian has a strong cubic term.¹⁰ The model of Baldereschi and Lipari, for shallow acceptor states, indicates that silicon is an anomalous host, as far as the semiconductors go, since the cubic term is large and cannot be treated well by their approach. This means that the total wave function of our problem (at least ignoring the coupling term) is also nearly even or odd, even though the point symmetry must be T_d .

We have explored many different values of the parame-

ters and can draw some definite conclusions from our analysis. It is apparent that in order to get parity to be nearly a good quantum number, *the minima must be well resolved in the $\langle 100 \rangle$ directions, although not necessarily deep.* The “bumps” in the potential, other than in the $\langle 100 \rangle$ directions, can still be important (maintaining T_d symmetry) unlike in the octahedral tunneling model. We have witnessed cases when the $\langle 100 \rangle$ directions were the global minima (although not the only minima) in which parity was not a good quantum number for any of the levels.¹² This again restricts the parameter space. We have also witnessed cases when parity is nearly a good quantum number in which certain levels were quite linear as a function of K , except when approaching very closely to one another. A classic “avoided crossing” was seen, again indicating that parity is not *exactly* a good quantum number.

Thus, at least qualitatively, parity considerations allow a strong sideband transition to the third rotational level, with only a weakly allowed transition to the intermediate T_2 level when coupling is introduced. We will quantitatively calculate oscillator strengths in Sec. IV, where coupling is included.

It has been shown, to this point, that the (H,Be) and (D,Be) complexes in silicon can be modeled using a rigid rotor in a tetrahedral field when the minima are in $\langle 100 \rangle$ directions. Indeed, using a C_4 and C_6 that give minima in the $\langle 100 \rangle$ direction with parity being nearly a good quantum number, K is determined by forcing the difference in dimensionless energy between the first and third rotational states to agree with experiment.

One problem remains, however. How are the stress results of Peale, Muro, and Sievers² explained? The fact that the largest effect is seen for [111] stress presumably points to $\langle 111 \rangle$ minima.

III. STRESS EFFECTS ON ROTATIONAL LEVELS

A. Tetrahedral tunneling model

We start our analysis with the tetrahedral tunneling model introduced by Haller, Joos, and Falicov, where two nuclear tunneling levels (A_1 and T_2) are predicted.³ Under [111] and [001] stress, the T_2 level is split into a twofold degenerate level and a nondegenerate level, while for [110] stress all degeneracies are removed, in principle.¹³ Peale, Muro, and Sievers have attempted to calculate the stress dependence in this limit.² However, an error was made, which weakens their argument in support of a $\langle 111 \rangle$ model.

It is assumed that the strain is small so that, to first order, the strain Hamiltonian is written as

$$\mathcal{H} = \sum_{i,j} V_{ij} \epsilon_{ij} , \quad (12)$$

where ϵ_{ij} is the strain tensor. We can put this equation into a more convenient form, as Ham did,¹⁴ as

$$\mathcal{H} = \sum_{i,j} \epsilon_{ij} (\Theta_d \delta_{ij} + \Theta_u \sum_I |\phi_I\rangle \langle \phi_I| n_i^I n_j^I) , \quad (13)$$

where Θ_d and Θ_u are nuclear strain-coupling coefficients, the ϕ 's are the four oriented $\langle 111 \rangle$ functions, and n_i^I is the i th component of the unit vector along the I direction. This form is completely analogous to that used for shallow donors in the effective-mass approximation, where the conduction-band minima are in four $\langle 111 \rangle$ directions for the host germanium and six $\langle 100 \rangle$ directions for silicon.

In Eq. (13), if i and j both range over $x, y,$ and z , meaning that both ϵ_{xy} and ϵ_{yx} appear in the sum, we find that the expressions for the energy eigenvalues given by Peale, Muro, and Sievers for [111] stress are correct, but for [110] they are incorrect. Since the strain tensor is a symmetric tensor and interchanging α and β does not affect the product $n_\alpha^I n_\beta^I$, having both ϵ_{xy} and ϵ_{yx} appear in the sum amounts to introducing a multiplicative factor of two. Some authors prefer to restrict the sum over (α, β) , so that only the upper triangle of the strain tensor appears in the sum. This amounts to redefining the deformation constants by a factor of two. A factor of two is missing for [110] stress. Ham's calculations support our assertion.¹⁴ The correct formula is presented here. Common constants (diagonal nuclear tunneling and the linear hydrostatic shift, due to uniaxial stress) have been subtracted for all levels and all stresses. For [111] stress, we find

$$\begin{aligned} E(A_1^{(1,2)}) &= f - t \pm 2\sqrt{t^2 + ft + f^2} , \\ E(E) &= -f + t , \end{aligned} \quad (14)$$

and for [110] stress,

$$\begin{aligned} E(A_1^{(1,2)}) &= -t \pm \sqrt{4t^2 + (\frac{3}{2}f)^2} , \\ E(B_1) &= t + \frac{3}{2}f , \\ E(B_2) &= t - \frac{3}{2}f , \end{aligned} \quad (15)$$

and for [001], there is no effect (other than the common hydrostatic shift). In these equations, $f = (\frac{1}{9})\Theta_u s_{44} P$, a stress parameter where P is the stress, negative for compression. Also, the notation is the usual for the groups C_{3v} and C_{2v} for [111] and [110] stress, respectively. Figure 2 displays the correct stress dependence, where the eigenvalues have been normalized to t , the tunneling matrix element.

There are several important points to make. Peale, Muro, and Sievers used the incorrect theoretical uniaxial stress results to justify a $\langle 111 \rangle$ tunneling model for the (H,Be) and (D,Be) complexes in silicon, even though a $\langle 111 \rangle$ model must be eliminated, because the values of the blueshifted replicas are larger than the free rotor limit, as discussed previously. Their reasoning is based on the fact that [111] stress has the “largest” effect, both experimentally and in their theoretical calculation.² Hence, the correct energy spectrum as given in the above equations and displayed in Fig. 2 weakens their argument, since the effects of [110] stress are larger than what was thought. Also, and this is an important point, one must be careful of the use of the word “largest.” Since this theoretical calculation involves *only* the nuclear rotational levels and not the entire problem including coupling, in

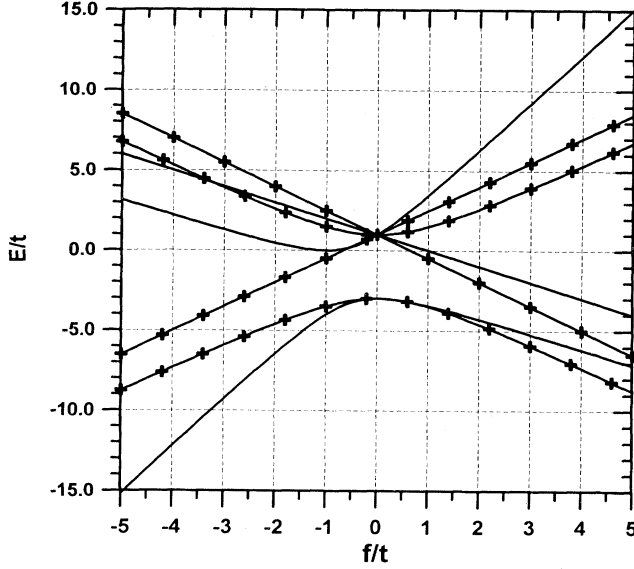


FIG. 2. The correct effects of uniaxial stress in the tetrahedral tunneling model, as given in Eqs. (14) and (15). The levels marked with “+” are for [110] stress, while the unmarked solid levels are for [111] stress. There is no effect, other than the hydrostatic shift, for [001] stress.

order to attempt a fit to experiment the *difference* between the experimental energy of the blueshifted replica (I^*) and the main band (I) must be taken, since the common hydrostatic shift and the stress effects on the coupled ground state are eliminated by this process. This difference in transition energies should, therefore, reflect only the character of the nuclear tunneling states in the excited p -like envelope acceptor states, where the coupling of the two degrees of freedom will be insignificant. Hence, the stress effects on the nuclear rotational tunneling levels should be isolated.

In fact, this is in essence what Peale, Muro, and Sievers did to extract one of the deformation potentials.² The difference in energy between the blueshifted replica and the mainband *decreases* slightly as the stress is increased, for all three stress directions.² The phrase “largest effect” should therefore mean, in application to the experiment, the largest decrease in separation of the calculated effects of uniaxial stress as shown in Fig. 2, not the largest curvature. Clearly then, [110] stress has the largest effect, at least for positive f/t .

To push this point a bit further, Peale, Muro, and Sievers show that for the largest stress allowed by their equipment for [111] stress, the quantity f in Eq. (14) has a maximum value of about 2 cm^{-1} . The difference between the two approaching levels (E and $A_1^{(1)}$) for positive f is about 0.91 of the difference between the unstressed levels, assuming $t = 4.05 \text{ cm}^{-1}$ as they did for the D isotope. Roughly speaking, then, the *difference* between the blueshifted replica and the mainband is nearly constant for all values of experimental stress. With experimental error considered, especially the error introduced due to the broadening of the I^* line, this indeed is a fair statement

for *all* the experimental principal stresses with the *same constant*. Since this is, in fact, the experimental case, it will be difficult to fit any nuclear tunneling model conclusively, or indeed all models, to the stress data. Larger stress values and higher resolution could solve this problem. Hence, the experimental stress data do not support a $\langle 111 \rangle$ model for these complexes.

B. Octahedral tunneling model

We will indicate the effects of stress within the octahedral tunneling model of Artacho and Falicov,⁵ since the results have not yet been published. We will find that what Peale, Muro, and Sievers argued intuitively is indeed correct.² That is, [001] stress produces the largest curvature with [110] stress being intermediate, while [111] stress has no effect other than the common hydrostatic shift.

The calculation is formally identical to the tetrahedral tunneling model, except now we have six $\langle 100 \rangle$ oriented functions. One finds linear combinations of these six functions that will block diagonalize the Hamiltonian.¹² For [001] stress, with the hydrostatic linear shift and diagonal nuclear energy subtracted, we find

$$E(A_{1g}^{(1,2)}) = -t - \frac{f'}{2} \pm \sqrt{\frac{9}{4}(f' - 2t)^2 + 6f't} ,$$

$$E(E_u) = f' ,$$

$$E(A_{2u}) = -2f' ,$$

$$E(B_{1g}) = 2t + f' .$$

(16)

We find for [110] stress the energy levels are given by

$$E(A_g^{(1,2)}) = \frac{f'}{4} - t \pm \left[9 \left(\frac{f'}{4} + t \right)^2 - 3f't \right]^{1/2} ,$$

$$E(B_{1u}) = f' ,$$

$$E(B_{2u}) = E(B_{3u}) = -\frac{f'}{2} ,$$

$$E(B_{1g}) = 2t - \frac{f'}{2} ,$$

(17)

where $f' = (\frac{1}{3})(s_{12} - s_{11}) \odot_u P$ for both sets, and P is negative for compression. The group theoretical notation is standard for the groups D_{4h} and D_{2h} for [001] and [110] stress, respectively. There is no effect for [111] stress, besides the hydrostatic shift.

For convenience in plotting we divide the above equations by t , the tunneling matrix element, and plot the levels as a function of f'/t in Fig. 3. Notice that the substitution $f' \rightarrow -f'/2$ converts all levels for [100] stress to [110] stress.

A fit could be attempted with this model also, since the difference in energy between the blueshifted replica and mainband is nearly constant, decreasing only very slightly for the three principal stresses.² From Fig. 3, for [001] stress this convergence could be fit, for positive f'/t , by a transition between the two A_{1g} levels, while for negative f'/t a transition from the ground A_{1g} to the excited acceptor state with B_{1g} tunneling symmetry would fit.

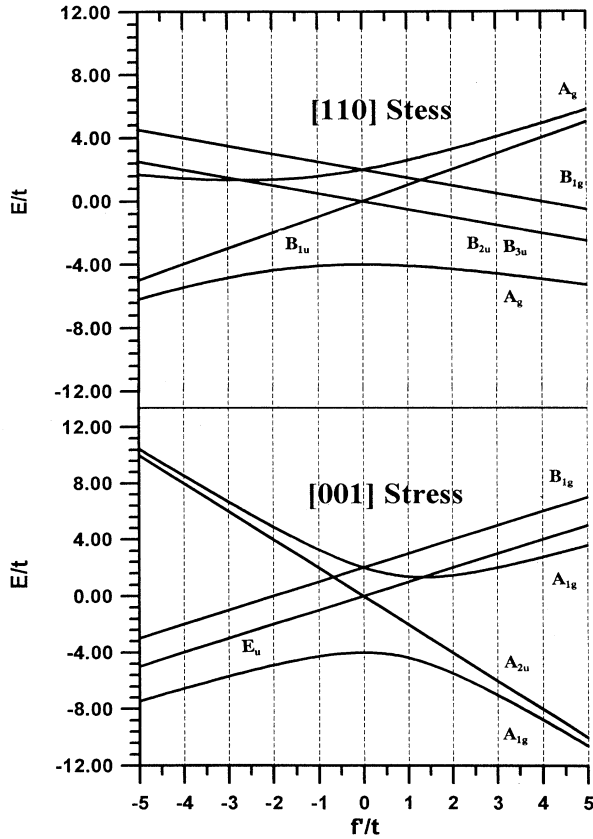


FIG. 3. The calculated uniaxial stress effects in the octahedral tunneling model, as given in Eqs. (16) and (17). The upper plot is for [110] stress and the lower plot is for [001] stress. There is no effect, other than the hydrostatic shift, for [111] stress.

Simultaneously, a fit to [110] stress would be possible for an A_g to B_{1g} transition for positive f'/t , and A_g to A_g for negative f'/t . Notice that for positive f'/t , this model would predict that for [001] stress the levels will initially converge, but will start to diverge for a value of f'/t equal to $\frac{2}{3}$, and for [110] stress the difference in energy between the blueshifted replica and the mainband would decrease asymptotically to $\frac{2}{3}$ of the unstressed difference. For negative f'/t , [110] stress will decrease the energy difference until f'/t reaches a value of $-\frac{4}{3}$, then the energy difference will increase indefinitely as the stress is increased, while for [001] stress the energy difference will decrease to $\frac{2}{3}$ of its initial value. This octahedral tunneling model predicts that the difference between the blueshifted replica and the mainband for [111] stress will stay constant, since there is no effect, other than the hydrostatic shift, in this model. However, the very slight convergence seen experimentally for [111] stress could be argued to originate from a small dependence of the stress behavior on the *excited* single acceptor state.

C. Rigid rotor in a tetrahedral field with $\langle 100 \rangle$ minima

We wish to develop a model that fits conveniently within the development of our rigid-rotor model.^{4,9,12} As

stress in some direction is applied to the system, the symmetry is reduced so that different terms, with lower L values, will appear in our expansion of spherical harmonics. The specific terms can be determined easily by group theory, since they must transform as A_1 in the reduced group, but we must apply physical arguments in order to determine which terms must be kept to be correct to first order. Also, the number of parameters can be reduced by utilizing physical arguments.

We write the Hamiltonian as

$$\mathcal{H} = \mathcal{H}_N(K, C_4, C_6) + \mathcal{H}' \quad (18)$$

where the first term reminds the reader that the rigid rotor in a tetrahedral field (expanded in spherical harmonics) depends upon three parameters, and \mathcal{H}' takes into account the stress. \mathcal{H}' is also expanded in spherical harmonics and will be diagonalized within a subset of the set of eigenstates of \mathcal{H}_N . Since the stress reduces the symmetry from T_d , spherical harmonics with less than $L=3$ will appear. By group theory, we can easily find the new terms. For [001], [110], and [111] stresses the sets $\{Y_{00}, Y_{20}, \dots\}$, $\{Y_{00}, Y_{10}, Y_{20}, i(Y_{22} - Y_{2-2}), \dots\}$, and $\{Y_{00}, [(i-1)Y_{11} + (i+1)Y_{1-1} + \sqrt{2}Y_{10}], [(i-1)Y_{21} + (i+1)Y_{2-1} + i(-Y_{22} + Y_{2-2})], \dots\}$ are allowed in the expansion, respectively. However, we are interested only in calculating the effects of stress to first order, since any experimental stress is small. Also, we do not wish to introduce a plethora of parameters. Both these considerations can be solved by using physical arguments.

The physical arguments we employ were motivated by an idea used by Watkins and Corbett for a different defect.¹⁵ The central idea is that the change in energy of a particular well, specifically in the $\langle 100 \rangle$ directions, is related to the strains along the lines connecting the four silicon nearest neighbors to each other. For example, consider the well in the [001] direction. This well straddles two silicon atoms. We are assuming that the change in energy of the [001] well, due to an imposed stress, is proportional to the fractional strain of these two silicon atoms along the line connecting them. These calculations have been done in great detail elsewhere.¹² We find that the stress Hamiltonians for the three principal stresses to first order assuming $\langle 100 \rangle$ minima are given by

$$\begin{aligned} \mathcal{H}_{[001]} &= -SY_{20}(\theta, \phi), \\ \mathcal{H}_{[110]} &= \frac{S}{2\beta} \{ Y_{10}(\theta, \phi) + \beta Y_{20}(\theta, \phi) \}, \\ \mathcal{H}_{[111]} &= \frac{S}{3\sqrt{2}\beta} \{ (i-1)Y_{11}(\theta, \phi) + (i+1)Y_{1-1}(\theta, \phi) \\ &\quad + \sqrt{2}Y_{10}(\theta, \phi) \}, \end{aligned} \quad (19)$$

where S is the single stress parameter introduced, given by

$$S = \frac{\alpha(s_{11} - s_{12})P}{3Y_{20}(\theta=0^\circ)} \quad (20)$$

Here, α is a proportionality constant relating the change in energy of a $\langle 100 \rangle$ well to the strain, P is the external stress (*positive* for compression), s_{11} and s_{12} are two of

the elastic compliance coefficients, and the Y is a spherical harmonic. β in Eq. (19) is a constant for a given host crystal, and is given by

$$\beta = \left[\frac{2Y_{10}(\theta=0^\circ)}{3Y_{20}(\theta=0^\circ)} \right] \left[\frac{s_{11}-s_{12}}{s_{44}} \right]. \quad (21)$$

We find that for silicon, using known values of s_{11} , s_{12} , and s_{44} for the perfect crystal,¹⁵ $\beta = +0.40$.

In the octahedral tunneling model, it was seen that [111] stress had no effect, other than a constant shift. One can see this physically by picturing the six $\langle 100 \rangle$ wells, and noting that [111] stress should affect each well the same way, so that only a shift in the energy levels should occur. However, notice that one is assuming O_h symmetry for the Hamiltonian. However, the present rigid-rotor calculation and stress analysis within this model are based upon T_d symmetry for the Hamiltonian, which is producing $\langle 100 \rangle$ minima. Visualizing the defect at a substitutional site with the four silicon nearest neighbors, one can clearly see that all six minima are *not* affected the same by the movement of the silicon atoms. Hence, the stress Hamiltonian as given in Eq. (19) for [111] stress is nonzero.

The appearance of $L=1$ terms in the Hamiltonians can be interpreted as a result of an induced electric field, due to the movement of the atoms. The point symmetry of a substitutional site in silicon is T_d , which does not include inversion.

Since Peale, Muro, and Sievers concentrated on the stress response of the (D,Be) complex in silicon,² we need to set K , C_4 , and C_6 in the rigid-rotor model, so that the energy levels correspond to this complex with $\langle 100 \rangle$ minima. C_4 and C_6 adjust the shape so that we are ensured $\langle 100 \rangle$ minima, and K is adjusted so that the energy difference between the first (A_1) and third (E) rotational levels agrees with experiment. For the (D,Be) complex, the dimensionless energy difference between the first and third levels must lie between 2.80 and 3.44 (center of mass, and Be fixed) if the bond length is nearly equal to the free result.

We set $C_4=2.0$ and $C_6=0.3$. For these values, the $\langle 100 \rangle$ directions are well-resolved minima. The $\langle 110 \rangle$ directions are slightly lower than the $\langle 111 \rangle$ (bonding) directions, so that the best tunneling paths are through the twelve $\langle 110 \rangle$ directions, which was suggested by other theoretical calculations.^{7,8} K is set to 8.5, which gives an energy difference between the first and third nuclear levels of 2.875. Figure 4 indicates the stress response of the first three levels to [001], [110], and [111] stress, using the above analysis. These plots were obtained by first diagonalizing \mathcal{H}_N in Eq. (18), using an expansion of spherical harmonics, up to and including $L=15$, then diagonalizing \mathcal{H}' as given in Eq. (19), using the first 36 eigenfunctions obtained from \mathcal{H}_N (using the full 256 expansion).

We will not attempt a fit to experiment, since this may be misleading for (at least) two reasons. First, we have not included here any coupling between the hole and the diatomic nuclei. This will affect the ground state from which a transition is being made. The calculations above are the effects on the nuclear levels only. Second, a fit

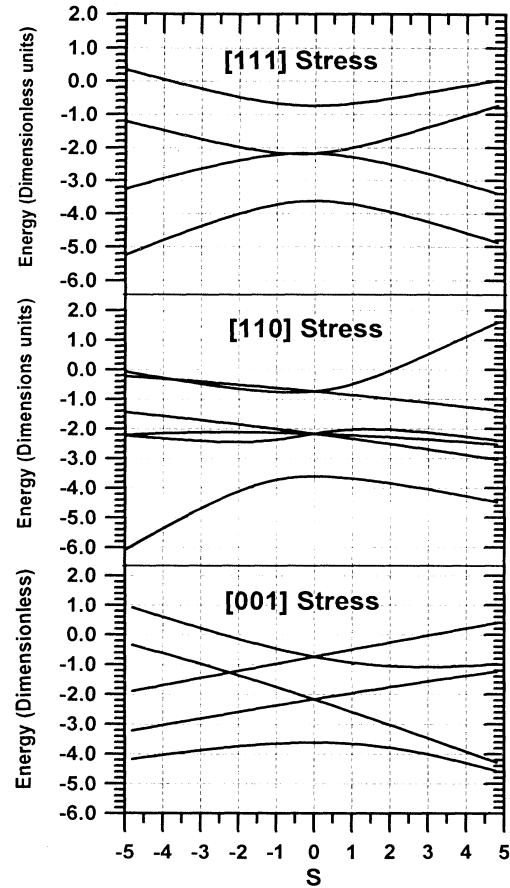


FIG. 4. The calculated effects of uniaxial stress within the model of a rigid rotor in a tetrahedral field with parameter values $K=8.5$, $C_4=2.0$, $C_6=0.30$, which are more appropriate for the deuterium isotope. With these values of the parameters, the global minima are in the six $\langle 100 \rangle$ directions, and parity is nearly a good quantum number for the levels shown. Unlike in the octahedral tunneling model, there are significant effects for [111] stress.

could be attempted by taking the difference between I and I^* , but as discussed before, the difference between these two peaks is nearly a constant for all directions and magnitudes of stress, making it difficult to fit conclusively. If a fit is attempted, it is implicitly assumed that the stress effect in the excited p -like envelope states is independent of the nuclear rotational tunneling state. Our main point in calculating the effects of stress on the rotational levels is to indicate that there are effects for [111] stress with $\langle 100 \rangle$ minima, dispelling the implicit assumption made that this was not the case. The stress results of Peale, Muro, and Sievers do not eliminate a $\langle 100 \rangle$ minima model.

IV. OSCILLATOR STRENGTHS IN THE INFRARED AND FAR INFRARED

A. Coupling

In order to calculate the oscillator strengths we now need to develop a scheme for coupling the hole motion

and rotational motion of the complex, V , as written in Eq. (1). General group theoretical arguments are used with some physical assumptions in order to obtain an expression for V .

We are interested in coupling the rotational tunneling nuclei only to a Γ_8 hole state, since it is assumed that only the s -like envelope ground state of \mathcal{H}_a (which is Γ_8) can couple significantly. Since this is the case, we look at the direct product

$$\Gamma_8 \otimes \Gamma_8 = \{\Gamma_1 + \Gamma_3 + \Gamma_5\} + \{\Gamma_2 + 2\Gamma_4 + \Gamma_5\}, \quad (22)$$

where the notation is standard for the cubic group.

It appears from Eq. (22) that one standard operator of each type Γ_1 , Γ_2 , and Γ_3 and two from Γ_4 and Γ_5 will be needed. However, this can be reduced by making reasonable assumptions. We assume V is real (only depending on the coordinates, not the momenta). Hence, only the *antisymmetric* part of the product in Eq. (22) is needed, which is the first bracketed term on the right. The second bracketed term on the right is the symmetric part. Therefore, the most general way of writing the interaction between the two degrees of freedom, so that the overall symmetry of the coupling is A_1 (or Γ_1) under simultaneous application of symmetry operators in both systems, is

$$\begin{aligned} V(\mathbf{r}, \mathbf{R}) = & V_1 T_1(\mathbf{r}) T_1(\mathbf{R}) \\ & + V_3 \{T_\theta(\mathbf{r}) T_\theta(\mathbf{R}) + T_\epsilon(\mathbf{r}) T_\epsilon(\mathbf{R})\} \\ & + V_5 \{T_x(\mathbf{r}) T_x(\mathbf{R}) + T_y(\mathbf{r}) T_y(\mathbf{R}) \\ & + T_z(\mathbf{r}) T_z(\mathbf{R})\}, \quad (23) \end{aligned}$$

where $\{T_1\}$ are Γ_1 , $\{T_\theta, T_\epsilon\}$ are Γ_3 , and $\{T_x, T_y, T_z\}$ are Γ_5 standard operators.¹⁶ All the T 's are Hermitian operators. The V 's are real constants. One must not confuse V_1 in this expression with Haller, Joos, and Falicov V_1 .³

The formalism is now complete. The goal is then to find all the possible nonzero matrix elements. For evaluating matrix elements of the hole (\mathbf{r}) standard operators within Γ_8 , any convenient representation of Γ_8 can be used. In particular,

$$\begin{aligned} |\frac{3}{2}, \frac{3}{2}\rangle &= -\frac{1}{\sqrt{2}}(X + iY)\uparrow, \\ |\frac{3}{2}, \frac{1}{2}\rangle &= \frac{1}{\sqrt{6}}[2Z\uparrow - (X + iY)\downarrow], \\ |\frac{3}{2}, -\frac{1}{2}\rangle &= \frac{1}{\sqrt{6}}[2Z\downarrow + (X - iY)\uparrow], \\ |\frac{3}{2}, -\frac{3}{2}\rangle &= \frac{1}{\sqrt{2}}(X - iY)\downarrow, \end{aligned} \quad (24)$$

where X , Y , and Z are any functions that transform as the x , y , and z coordinates, respectively, and the arrows correspond to spinors for a spin of $\frac{1}{2}$.¹⁷ Any proportionality constants can be absorbed into the definitions of V_1 , V_3 , and V_5 .

Using Eq. (24) as representations of the four Γ_8 ground

hole states, we project out of V the hole part. This four by four submatrix is given by

$$\langle m | V(\mathbf{r}, \mathbf{R}) | m' \rangle = \begin{pmatrix} a+b & c^* & d^* & 0 \\ c & a-b & 0 & d^* \\ d & 0 & a-b & -c^* \\ 0 & d & -c & a-b \end{pmatrix}, \quad (25)$$

where m and m' label the four hole states, and

$$\begin{aligned} a &= V_1 T_1(\mathbf{R}), \quad b = V_3 T_\theta(\mathbf{R}), \\ c^* &= \frac{V_5}{\sqrt{3}} [iT_x(\mathbf{R}) - T_y(\mathbf{R})], \quad d^* = V_3 T_\epsilon(\mathbf{R}) + i \frac{V_5}{\sqrt{3}} T_z(\mathbf{R}), \end{aligned} \quad (26)$$

where the T 's are operators which operate only on the rotor's coordinate, and the V 's are real parameters. It is interesting to note that from a symmetry point of view, this problem is similar to that treated by Rodriguez, Fisher, and Barra, where they considered the splitting of the double-valued representations in T_d under stress.¹⁸ Their Tables III and IV are analogous to Eq. (25).

Since " a " is along each diagonal element and it is diagonal in \mathbf{R} space (the rotor's coordinate), it will just shift the centroid of energy. We, therefore, ignore it when calculations are made.

We wish to incorporate this additional 4 by 4 "potential" in our rigid-rotor model. To first order, we will again use spherical harmonics to represent the T 's in Eqs. (25) and (26). The set $\{T_x, T_y, T_z\}$ transforms as T_2 , so that the harmonics with lowest L that transform as this set are the three $L=1$ functions. However, the Γ_8 hole states are associated with the Bloch functions at the top of the valence band, which are predominantly of p -like character. Since the envelope functions of these states are s like, the overall character of the Γ_8 states near the origin will be governed by the p -like character of the Bloch functions. This means, to lowest order, that only an even function can connect the four Γ_8 states. Hence, the set $\{T_x, T_y, T_z\}$ will be best represented by $L=2$ spherical harmonics, namely, those that transform as $\{xy, xz, yz\}$.

There is a more intuitive and physical way to approach this problem without resorting to symmetry arguments. Its essence is to assume a Columbic interaction between the hole and rotor. All sixteen products of the four Γ_8 representation functions as given in Eq. (24) are found, and then used to define a matrix. The diagonal elements of this matrix are then the probability densities of each state. One can then use the expression

$$\frac{1}{r_{12}} = 4\pi \sum_L \sum_M \frac{1}{2L+1} \frac{r_{<}^L}{r_{>}^{L+1}} Y_{LM}(\theta_1, \phi_1) Y_{LM}^*(\theta_2, \phi_2), \quad (27)$$

for integrating over the hole coordinate. One finds a final four by four matrix identical to the one derived by symmetry arguments if one lets $V_3 = -V_5/\sqrt{3}$ in Eq. (26). Finally, then, the four by four submatrix is given by

$$\langle m|V(\mathbf{r},\mathbf{R})|m'\rangle = \begin{pmatrix} \eta Y_{00} - \xi Y_{20} & \sqrt{2}\xi Y_{21}^* & -\sqrt{2}\xi Y_{22}^* & 0 \\ \sqrt{2}\xi Y_{21} & \eta Y_{00} + \xi Y_{20} & 0 & -\sqrt{2}\xi Y_{22}^* \\ -\sqrt{2}\xi Y_{22} & 0 & \eta Y_{00} + \xi Y_{20} & -\sqrt{2}\xi Y_{21}^* \\ 0 & -\sqrt{2}\xi Y_{22} & -\sqrt{2}\xi Y_{21} & \eta Y_{00} - \xi Y_{20} \end{pmatrix}, \quad (28)$$

where $\{\eta, \xi\}$ are real parameters, and all the $L=2$ harmonics are functions of the rotor's coordinates. This form lends itself rather nicely to our algorithm. We first diagonalize $\mathcal{H}_N(K, C_4, C_6)$, using as basis functions the spherical harmonics up to and including $L=15$, then "squeeze" Eq. (28) on both sides with the eigenvectors gotten from the first diagonalization. We will use only a subset of all the eigenvectors (typically the first 25 or 36, resulting in a final diagonalization of 100 by 100 or 144 by 144 matrix) from \mathcal{H}_N , so that this is a perturbative calculation (however, much better than first order) for the coupling.

The model of Haller, Joos, and Falicov, for coupling in the tetrahedral tunneling model,³ and as later used in the octahedral tunneling model by Artacho and Falicov,⁵ is also a two parameter coupling scheme. However, their two parameters are of mixed symmetry. Our coupling scheme, however, contains one parameter (η), which is purely $\Gamma_1 (A_1)$ and another (ξ), which contains contributions from both $\Gamma_3 (E)$ and $\Gamma_5 (T_2)$. Since the Γ_1 part only shifts the centroid of energy, the splittings can be plotted versus one parameter, thus simplifying the analysis.

Without the coupling term V , the total Hamiltonian (T_d symmetry) is invariant under operators which operate independently either on the hole's coordinate or the rotor's coordinate. With the addition of V , the Hamiltonian is invariant under simultaneous application of a specific operator on both coordinates. Hence, there is a reduction of symmetry, so that the uncoupled levels will split. All possible reductions in T_d symmetry when the coupling is to a Γ_8 hole state are

$$\begin{aligned} A_1 \otimes \Gamma_8 &\rightarrow \Gamma_8, & A_2 \otimes \Gamma_8 &\rightarrow \Gamma_8, & E \otimes \Gamma_8 &\rightarrow \Gamma_6 \oplus \Gamma_7 \oplus \Gamma_8, \\ T_1 \otimes \Gamma_8 &\rightarrow \Gamma_6 \oplus \Gamma_7 \oplus 2\Gamma_8, & T_2 \otimes \Gamma_8 &\rightarrow \Gamma_6 \oplus \Gamma_7 \oplus 2\Gamma_8. \end{aligned} \quad (29)$$

Both Γ_6 and Γ_7 are twofold degenerate, while Γ_8 is fourfold degenerate.

The notation in Eq. (29) and in all following discussions will be as follows. We use the A, E, T notation when referring to the rotor degree of freedom, and we will use the "gamma" notation when referring to the hole, or the total, coupled system. Clearly, since the hole must be labeled with the double-valued representations of T_d ($\Gamma_6, \Gamma_7, \Gamma_8$) and the rotor with the single-valued representations, the total wave functions must transform as the double-valued representations.

B. Infrared oscillator strengths

We now have all the machinery to calculate oscillator strengths, and we will start with the infrared. It may

seem at this point that we have too many parameters to deal with effectively. However, the range of these parameters is severely restricted as has been indicated throughout this paper, for at least three of the four parameters (three from the rigid-rotor Hamiltonian and one nontrivial one from our coupling scheme). We have been able to find good agreement in transition energies and oscillator strengths for the (H,Be) isotope in both the far infrared and the infrared with the same set of parameters, with some additional features. The values of the parameters are $K=4.2$, $C_4=2.5$, $C_6=0.4$, and $\xi=-3.5$. These values give the correct spacing between the blueshifted replicas and the mainband, assuming that the bond length of the hindered rotor is near the free value. The value of the mixing parameter given predicts two strong transitions in the far infrared with the correct energy as found by Muro and Sievers experimentally, and an additional third strong transition, at an energy which is very sensitive to slight changes in the mixing parameter ξ .

The three parameters for the potential of the rigid rotor are quite reasonable, meaning that the expansion dies off quickly, justifying our neglect of terms higher than $L=6$, and the roughly equal strength of the $L=3$ and 4 term can be supported by the fact that the second- and third-nearest neighbors of the tumbling rotor impose O_h symmetry. All following data, including the next section, are calculations using the above values of the parameters. Figure 5 shows a general energy-level diagram with some transitions labeled indicating their expected strengths, with the values of the above parameters in mind. There are, of course, other additional levels in our calculation at higher energies, but we concentrate on the first three rotational levels in each acceptor state. It is possible that infrared transitions exist higher in energy to these additional levels, but we have not calculated them.

It is assumed for the hole transitions with nuclear rotational blueshifted sidebands (infrared) that the strength of the transition is primarily controlled by rotational overlap. The ground state is coupled so that the various pure rotational states are mixed in (i.e., different irreducible representations). The excited states, however, are assumed not to mix, so that the wave functions are simple products of hole functions and pure rotational states. Without the mixing in the ground state, only a dipole transition to an excited hole state with A_1 nuclear symmetry would be allowed.

If the *ratio* of the square of the rotational overlap is taken, then hole integrals that cannot be calculated will cancel. We, therefore, divide by the oscillator strength of the mainband (defined to be strength 1), here taken as a transition to the excited p -like hole level with A_1 rotational character. Also, since the energy of the hole tran-

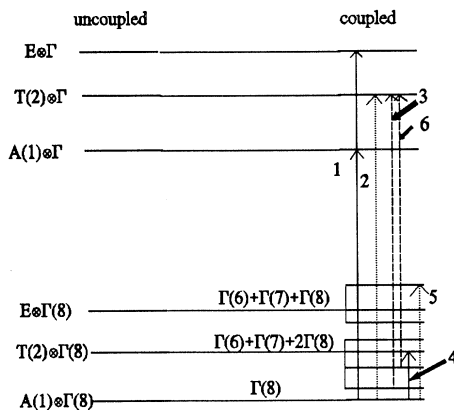


FIG. 5. Schematic energy-level diagram in the rigid-rotor model, with and without coupling between the rotor and hole. The lower set of levels have s -like envelope single acceptor states with Γ_8 symmetry, and the upper set of levels have single acceptor states, which transform as Γ with p -like envelopes. Both strong (solid or dashed) and weak (dotted) transitions are shown. Transitions labeled 1, 2, 3, and 6 are infrared transitions, while 4 and 5 are far-infrared transitions. The subscripts have been written in parentheses for clarity.

sition is much larger than the energy differences between the low-lying rotational levels, the energy-level difference factor in the definition of the oscillator strength is not important, so we ignore it in this case. We sum over the excited states and average over the ground level.

If parity were exactly a good quantum number as in the octahedral tunneling model or in the rigid-rotor model with extreme choices of the parameters, the oscillator strength to the intermediate T_{1u} level would be strictly zero. Of course, in the general case within our model, this is not the case. We, therefore, calculate the oscillator strengths of transitions to the intermediate T_2 level and to the E level, which we believe to be responsible for the blueshifted replicas. The strength of the T_2 transition must be small compared to the E transition.

We take into account population effects due to finite temperatures, since both Muro and Sievers,¹ and Peale, Muro, and Sievers² exhibited temperature-dependent spectra. We use the appropriate Boltzmann factors, and have carefully taken into account the degeneracies, and assume Gaussian linewidths. As indicated in Fig. 5 transitions 3 and 6 should be the strongest transitions from the initial levels indicated, since both the initial and final levels have T_2 character. We have calculated the oscillator strengths to the A_1 and E final levels, and include them in our calculation. However, the transitions from the second level in the coupled manifold, which is two-fold degenerate for $\xi = -3.5$, to these two excited states are very small.

Figure 6 shows the infrared absorption for the temperatures $T = 1.7, 8,$ and 15 K (displaced upwards each by 0.2 for clarity). The peak of the mainband is defined to be one at an energy of zero. The peaks are labeled as in

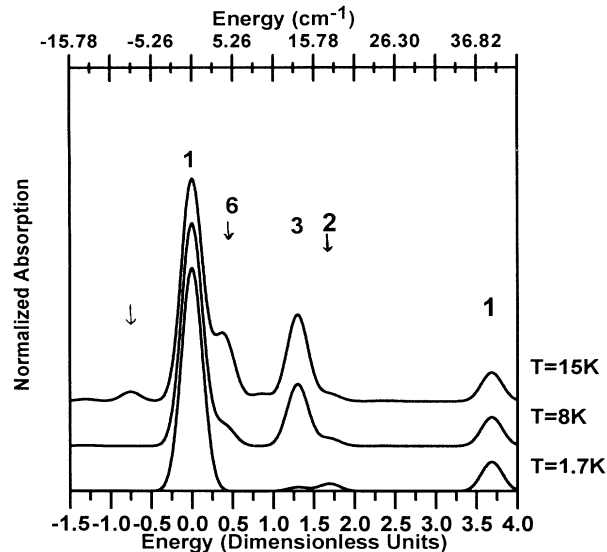


FIG. 6. Infrared absorption as predicted in the rigid rotor in a tetrahedral field model for $T = 1.7, 8,$ and 15 K, with parameter values $K = 4.2, C_4 = 2.5, C_6 = 0.4,$ and $\xi = -3.5$, so that the predicted spectrum should correspond to the $(\text{H,Be})^-$ complex in silicon. Various peaks are labeled as in Fig. 5. The three spectra for different temperatures are offset slightly for clarity. The peak at a dimensionless energy of 0.0 has a peak absorption defined to be 1. The lower-energy scale is in dimensionless units, which is scaled to the rotational constant B as in Eq. (3). The upper energy scale is in cm^{-1} , assuming that the rotational constant is near the free value of the $(\text{H,Be})^-$ molecule. Table I gives numeric data for this plot.

Fig. 5. We list in Table I the stronger transitions as labeled in Fig. 5. By definition, the blueshifted replica around 3.7 in dimensionless units is 38.8 cm^{-1} in wave-number units.

At $T = 1.7$ K, there is some structure between the mainband and the blueshifted replica, due to a transition to the intermediate T_2 nuclear character excited hole level, indicating that parity is not a perfect quantum number, and a small population is present, even at this low temperature, in the first excited level of the ground-state manifold. As the temperature increases, additional structure appears between the mainband and the blueshifted replica. It must be pointed out that this structure is mainly due to transitions to the intermediate T_2 nuclear character excited hole state, since the first few excited levels in the ground state manifold originate from the uncoupled T_2 level. The small peak between transitions 6 and 3 results from the fourth level in the coupled manifold, which originates from the E uncoupled level, to the E nuclear character excited state. We also indicate with an arrow in Fig. 6, some structure on the low-energy side.

C. Far-infrared oscillator strengths

We now calculate the oscillator strengths for transitions within the coupled ground-state manifold for the s -like envelope acceptor states. It is expected that strong

TABLE I. Selected information for our theoretical infrared transitions. "Peak value" means the oscillator strength calculated without regard to population effects. The labeling of the transitions is as in Fig. 5.

Transition No.	Transition energy (dimensionless)	Transition energy (cm ⁻¹)	Peak value
1 (lower)	≡ 0	0	≡ 1.0
1 (upper)	3.6851	38.8	0.1234
2	1.6927	17.8	0.0334
3	1.2995	13.7	0.5912
6	0.3823	4.0	1.1205

transitions occur between opposite parity nuclear states, since these transitions are within the same hole state.

For the far-infrared transitions, we will proceed with more detail to expose clearly our assumptions. The wave function for a state in the coupled manifold, which transforms as the irreducible representation Γ_i , is written as

$$\psi_{\Gamma_i}^\alpha = \left\{ \sum_m |\Gamma_8, m\rangle \sum_\Gamma \sum_j c_{\Gamma_j, m}^{\alpha, i} \phi_{\Gamma_j} \right\} F_s, \quad (30)$$

where the kets are the hole Bloch functions from the top of the valence band (Γ_8), the ϕ 's are nuclear rotational functions, which transform as irreducible representations of T_d , and F_s is the s -like envelope function. α is the degeneracy label. The sum over Γ is over irreducible representations and the sum j is over partners of Γ . We ultimately express the ϕ 's in terms of spherical harmonics, so that Eq. (30) becomes

$$\psi_{\Gamma_i}^\alpha = \left\{ \sum_m |\Gamma_8, m\rangle \sum_{L, M} a_{LM, m}^{\alpha, i} Y_{LM}(\hat{\mathbf{R}}) \right\} F_s, \quad (31)$$

where the expansion coefficients "a" are given by our algorithm, and \mathbf{R} is the coordinate of the rotor. We wish to calculate the oscillator strength of a transition from the ground state (which in our calculation is always Γ_8) to any of the coupled states Γ_i . It is assumed that for the dipole operator, the coordinate of the rotor (\mathbf{R}) is appropriate and that the light is polarized in the z direction. If \mathbf{R} is written in terms of its "spherical coordinates," the oscillator strengths become

$$f_{\Gamma_i} \propto (W_{\Gamma_i} - W_{\Gamma_8}) \langle \Gamma_8 | Y_{10}(\hat{\mathbf{R}}) | \Gamma_i \rangle|^2, \quad (32)$$

where the first term is the dimensionless energy difference between the two states. We will eventually take a ratio, so that any proportionality constant will cancel. Since the Y_{10} term in the dipole matrix element only depends on the rotor's coordinate and the hole wave functions are orthogonal, the dipole matrix element becomes

$$\langle \Gamma_8 | Y_{10}(\mathbf{R}) | \Gamma_i \rangle = \sum_m \sum_{LM} \sum_{L'M'} (a_{LM, m}^{\alpha, i})^* a_{L'M', m}^{\alpha', i} \int Y_{LM}^* Y_{10} Y_{L'M'} d\hat{\mathbf{R}}, \quad (33)$$

which is quite calculable within our algorithm. Finally, once the dipole matrix element is calculated using Eq.

(33), it is squared, then summed properly over the degeneracies of the levels involved.

We have elsewhere thoroughly checked our algorithm against the analytical expressions for the oscillator strengths that can be derived in the octahedral tunneling limit, with no disagreement found.¹² Figure 7 shows the theoretical far-infrared absorption spectra at $T=0$ K (the experiment is at 1.2 K), using the rigid-rotor model where we have assumed Gaussian linewidths, and have used normalized energy units. "1" in these units is defined to be the difference in energy between the first and third nuclear levels (uncoupled), which we have set to a value appropriate for the (H,Be) isotope. Table II indicates the energies and peak values of all seven transitions.

We indicate in Fig. 7 the three transitions to levels originating from the uncoupled level of E nuclear symmetry. As stated previously, in the octahedral tunneling model, these three transitions would be zero. They are weak here, especially the highest in energy, but are

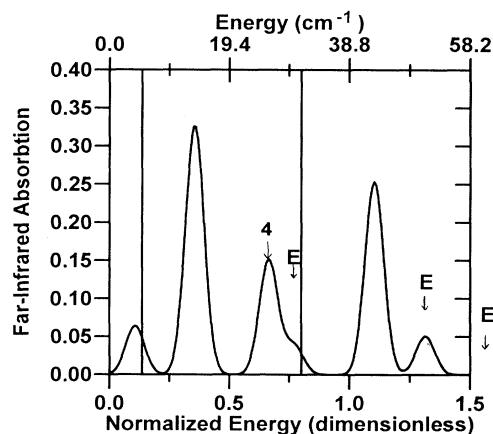


FIG. 7. Far-infrared spectrum predicted in our model with parameter values $K=4.2$, $C_4=2.5$, $C_6=0.4$, and $\xi=-3.5$. The energy scaling is such that 1 dimensionless unit = 38.8 cm⁻¹, shown in the lower and upper axes, respectively. The rotational constant B is assumed near the value of free rotation of the (H,Be)⁻ molecule. We indicate the peaks to the levels originating from the E uncoupled hindered rotor levels. Also, transition 4 as shown in Fig. 5 is indicated here. The box in normalized energy between about 0.2 and 0.8, indicates the published window of Muro and Sievers (Ref. 1).

TABLE II. Information on theoretical far-infrared transitions. The transition energies in cm^{-1} are calculated by assuming that the rotational constant B is nearly equal to the free value for $(\text{H,Be})^-$.

Transition number	Transition energy (dimensionless)	Transition energy (cm^{-1})	Degeneracy and nuclear character of upper level	Peak value
1	0.1067	4.1	2 (T_2)	0.0647
2	0.3556	13.8	4 (T_2)	0.3275
3	0.6645	25.8	2 (T_2)	0.1509
4	0.7694	29.9	2 (E)	0.0385
5	1.1042	42.8	4 (T_2)	0.2535
6	1.3154	51.0	4 (E)	0.0508
7	1.5625	60.6	2 (E)	0.0014

nonzero. The box indicates roughly the range of energies, which Muro and Sievers experimentally explored.¹ The fit is excellent within this window. We have two large absorption peaks in this window at the correct energies, and a third nearly hidden by the second smaller peak, all of which are relatively insensitive to small changes in the value of ξ . It is interesting to note that this nearly hidden peak is a transition to a level originating from the E rotational manifold. This at least qualitatively explains why the third peak seen by Muro and Sievers for the hydrogen isotope was too weak for them to identify precisely.¹

We also predict a transition at a lower energy (in energy units, at about 4 cm^{-1}), and a rather strong transition to a Γ_8 level at a higher energy (around 43 cm^{-1}). The specific value of the energy of transition for this strong, higher-energy transition is very sensitive to small changes in the value of the mixing parameter ξ . As ξ becomes more negative, the energy 43 cm^{-1} increases rapidly. This may be significant because, after completing these calculations, we learned of recent experiments¹⁹ over a broader energy range in which such a higher-energy transition was not observed. Thus, the optimal values of the parameters, particularly ξ , will be somewhat different from those given above.

V. CONCLUSION

We conclude that any model, which has the $\langle 111 \rangle$ directions (either bonding or antibonding) as minima or tunneling sites, is inadequate to model the (H,Be) and (D,Be) complexes in silicon. The major contradiction for this model is the fact that the energy values of the blueshifted replicas relative to the mainband seen in the infrared transitions are larger than the free rotor limit for the molecules. As has been shown, any potential must decrease the energy separation of the first two levels of the free rotor.⁴ However, the stress results seemed to initially support a $\langle 111 \rangle$ model, even with the above problem known. We believe, however, that if the stress results are looked at more carefully, the evidence is not conclusive. The central problem is that the difference in energy between the transition to the blueshifted replica and the transition to the mainband is nearly constant, only

slightly decreasing with applied stress. This makes it difficult to fit to any model conclusively. Better resolution and higher stress values could shed more light as to the nature of these problems.

Beyond the factual information that a $\langle 111 \rangle$ tunneling model must be eliminated, are the conceptual problems if such a model is incorporated. It is hard to imagine a system tunneling between bonding directions with a high-frequency rate when the breaking of bonds and large relaxations of the cage must most likely be occurring. The physics of semiconductors simply makes it difficult for such a system to exist, and is probably the main reason that it has only been recently that such systems have been actively searched for.

However, in T_d symmetry the six $\langle 100 \rangle$ directions are also possible minima sites. In fact, this is the only other possibility in T_d other than the two sets of $\langle 111 \rangle$ directions, as we have shown in the model of a rigid rotor in a tetrahedral field. We believe this paper has shown that the (H,Be) and (D,Be) complexes in silicon are most likely $\langle 100 \rangle$ rotationally tunneling defects. The contradiction in the $\langle 111 \rangle$ model in regard to the blueshifted replicas is completely eliminated when the minima are in $\langle 100 \rangle$ directions. The reason for this is that the third nuclear rotational level is responsible for the sidebands. Since the third level originates from the $L=2$ free rotor level, there is no contradiction. As we have indicated, as long as the potential of the rigid rotor has global minima in the $\langle 100 \rangle$ directions (determined by the parameters C_4 and C_6), there must be a value of K , such that the separation between the first and third levels agrees with experiment, and parity is nearly a good quantum number in our rigid-rotor model without assuming O_h symmetry for the Hamiltonian as Artacho and Falicov had to, within their small basis set octahedral tunneling model.

The major objection raised to a $\langle 100 \rangle$ model had been the experimental stress results. It was assumed that $[111]$ stress with $\langle 100 \rangle$ minima would not produce any effect. However, as shown herein, this is not the case in our rigid-rotor model. The reasoning for deducing that $[111]$ stress has no effect, other than the hydrostatic shift, when the system is tunneling between six $\langle 100 \rangle$ directions, is based on the assumption that the Hamiltonian describing the system is invariant under O_h symmetry. Such is the

case in the octahedral tunneling model proposed by Artacho and Falicov.⁵ However, we showed that if one assumes T_d symmetry for the Hamiltonian, which is inherent in our model, then [111] stress *does* have an effect when the minima are $\langle 100 \rangle$ directions, even though parity is nearly a good quantum number in the first three levels. Hence, the objection to a $\langle 100 \rangle$ minima model because of the experimental stress results is eliminated. Also, as indicated above, we believe the experimental stress results are not adequate to confirm a specific nuclear model.

Finally, our calculations of the oscillator strengths of transitions in both the infrared and far infrared assuming a consistent set of values of parameters in our rigid-rotor model, which are reasonable and give $\langle 100 \rangle$ minima, reproduce fairly well the known experimental absorption.

ACKNOWLEDGMENTS

The authors wish to thank Dr. F. S. Ham for his generous help in the symmetry-related problems of this research. We thank A. J. Sievers for comments on the manuscript and for continued interest in this problem. Also, thanks go to Dr. Gary G. DeLeo for his support and help over the past six years. Finally, the first author would like to express his gratitude to Holmes Community College, its President Dr. Starkey Morgan, the Vice President of the Ridgeland campus Mr. Joe Adams, and several of its faculty members for being very generous in a time when generosity was needed. This research was supported in part by the U.S. Navy Office of Naval Research (Electronics and Solid State Sciences Program), Contract No. N00014-89-J-1223.

*Current address: H C C-Ridgeland, Math/Science Department, 412 W. Ridgeland Ave., Ridgeland, MS 39157.

¹K. Muro and A. J. Sievers, Phys. Rev. Lett. **57**, 897 (1986).

²R. E. Peale, K. Muro, and A. J. Sievers, Phys. Rev. B **41**, 5881 (1990).

³E. E. Haller, B. Joos, and L. M. Falicov, Phys. Rev. B **21**, 4729 (1980).

⁴Kevin R. Martin and W. Beall Fowler, Phys. Rev. B **44**, 1092 (1991).

⁵Emilio Artacho and L. M. Falicov, Phys. Rev. B **43**, 12 507 (1991).

⁶P. J. H. Denteneer, C. G. Van de Walle, and S. T. Pantelides, Phys. Rev. Lett. **62**, 1884 (1989).

⁷L. S. Chia, N. K. Goh, and C. K. Ong, J. Phys. Chem. Solids **53**, 585 (1992).

⁸In-Ho Lee, B. H. Cheong, and K. J. Chang, Phys. Rev. B **46**, 2041 (1992).

⁹Kevin R. Martin, W. Beall Fowler, and Gary G. DeLeo,

Mater. Sci. Forum **83-87**, 69 (1992).

¹⁰A. Baldereschi and Nuncio O. Lipari, Phys. Rev. B **9**, 1525 (1974).

¹¹A. F. Devonshire, Proc. R. Soc. London Ser. A **153**, 601 (1936).

¹²Kevin R. Martin, Ph.D. Dissertation, Lehigh University, 1993.

¹³See, for example, M. Tinkham, *Group Theory and Quantum Mechanics* (McGraw-Hill, New York, 1964).

¹⁴F. S. Ham, Phys. Rev. B **38**, 5474 (1988).

¹⁵G. D. Watkins and J. W. Corbett, Phys. Rev. **121**, 1001 (1961).

¹⁶Frank S. Ham (private communication).

¹⁷See, for example, G. F. Koster, J. O. Dimmock, R. G. Wheeler, and H. Statz, *Properties of the Thirty-two Point Groups* (MIT, Cambridge, MA, 1966).

¹⁸Sergio Rodriguez, P. Fisher, and Fernando Barra, Phys. Rev. B **5**, 2219 (1972).

¹⁹A. J. Sievers (private communication).